

## Accepted Article

**Title:** Divergent Construction of Cyclobutane-Fused Pentacyclic Scaffolds via Double Dearomative Photocycloaddition

**Authors:** Ting-Ting Song, Fan Lin, Shan-Tong Xu, Bo-Chao Zhou, Li-Ming Zhang, Shi-Yu Guo, Xinglong Zhang, and Qing-An Chen

This manuscript has been accepted after peer review and appears as an Accepted Article online prior to editing, proofing, and formal publication of the final Version of Record (VoR). The VoR will be published online in Early View as soon as possible and may be different to this Accepted Article as a result of editing. Readers should obtain the VoR from the journal website shown below when it is published to ensure accuracy of information. The authors are responsible for the content of this Accepted Article.

**To be cited as:** *Angew. Chem. Int. Ed.* **2025**, e202505906

**Link to VoR:** <https://doi.org/10.1002/anie.202505906>

# Divergent Construction of Cyclobutane-Fused Pentacyclic Scaffolds via Double Dearomative Photocycloaddition

Ting-Ting Song,<sup>1</sup> Fan Lin,<sup>1</sup> Shan-Tong Xu,<sup>1</sup> Bo-Chao Zhou,<sup>1,2</sup> Li-Ming Zhang,<sup>1,2</sup> Shi-Yu Guo,<sup>1</sup> Xinglong Zhang,<sup>3\*</sup> Qing-An Chen<sup>1,2,\*</sup>

<sup>1</sup>Dalian Institute of Chemical Physics, Chinese Academy of Sciences, 457 Zhongshan Road, Dalian 116023, China

<sup>2</sup>University of Chinese Academy of Sciences, Beijing 100049, China

<sup>3</sup>Department of Chemistry, The Chinese University of Hong Kong, Shatin, New Territories, Hong Kong, China

\*Corresponding author E-mail: xinglong.zhang@cuhk.edu.hk, qachen@dicp.ac.cn

## Abstract

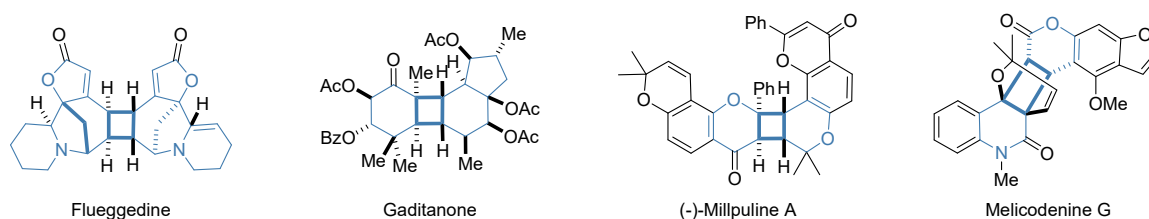
Cyclobutane-fused polycyclic scaffolds are structurally interesting cores in natural product synthesis and drug discovery. The construction of these skeletons often requires elaborate synthetic effort and gives low efficiency. We herein demonstrated the divergent construction of various cyclobutane-fused 2D/3D pentacyclic scaffolds by a photocatalytic intermolecular double dearomative cycloaddition of arenes. These skeletons, typically unattainable under thermal conditions, could be accessed with exclusive diastereoselectivity under mild photochemical conditions. Combined experimental and computational mechanistic studies elucidate that the reaction proceeds through a cascade sequence involving photocatalytic 1,4-hydroalkylation, alkene isomerization, and [2+2] cycloaddition via an intertwined single electron transfer (SET)/energy transfer (EnT) nature. This protocol provided a divergent synthetic approach for constructing (pseudo)-dimeric cyclobutane-fused 2D/3D pentacyclic scaffolds. The visible-light-induced intermolecular double dearomative cycloaddition between naphthalenes and benzothiophenes was also realized, providing indispensable methods for unprecedented structurally diverse polycyclic molecules that were difficult to access by conventional transformations.

## Introduction

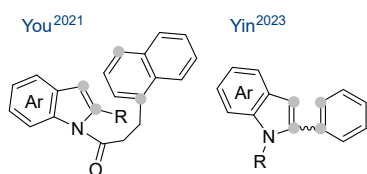
Cyclobutane-fused polycyclic skeletons, possessing idiosyncratic and infrequent structural and physicochemical properties, have emerged as important scaffolds in many biologically active and medicinally valuable natural products (Fig. 1A).<sup>[1]</sup> For example, flueggidine, a new dimeric Securinega alkaloid with a unique highly symmetrical skeleton, was isolated and possessed potential pharmacological activity.<sup>[2]</sup> As an important diterpenoid with an unprecedented 5-6-4-6-fused tetracyclic ring skeleton, gaditanon has potential biological activity in terms of PKC activation.<sup>[3]</sup> Additionally, (-)-millipuline A, which bears a flavonoid dimer skeleton that is constructed by a cyclobutane linked to a

pyran ring and  $\gamma$ -pyrone ring, displayed a suppressive effect in miR-144 expression.<sup>[4]</sup> The naturally occurring quinolinone-coumarin [2+2] cycloadduct, melicodenine G, showed potent antiproliferative activity against DLD-1 colon cancer cells by inducing apoptosis.<sup>[5]</sup> However, the preparation of such polycyclic molecules featuring high ring strain often requires elaborate synthetic effort from pre-functionalized substrates with low step economy. Therefore, the advancement of general and straightforward synthetic methods towards cyclobutane-fused polycyclic scaffolds from readily available feedstock resources with high reaction efficiency/selectivity is highly desirable.

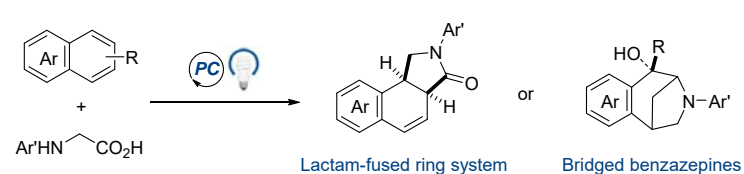
### A Representative bioactive molecules with cyclobutane-fused polycyclic scaffolds



### B Double dearomative cycloaddition of arenes



### C Previous work: Photoredox-catalyzed intermolecular dearomatization of arenes



### D Challenges and strategy for the synthesis of cyclobutane-fused pentacyclic scaffolds

#### Regioselectivity



#### Diastereoselectivity



#### Challenges:

- ⊕ Harsh conditions
- ⊕ Regioselectivity regulation
- ⊕ Diastereoselectivity regulation

#### Strategy:

- ⊕ Mild conditions
- ⊕ Radical precursor (R')
- ⊕ SET/EnT cascade process

### E This work: Divergent construction of cyclobutane-fused pentacyclic scaffolds

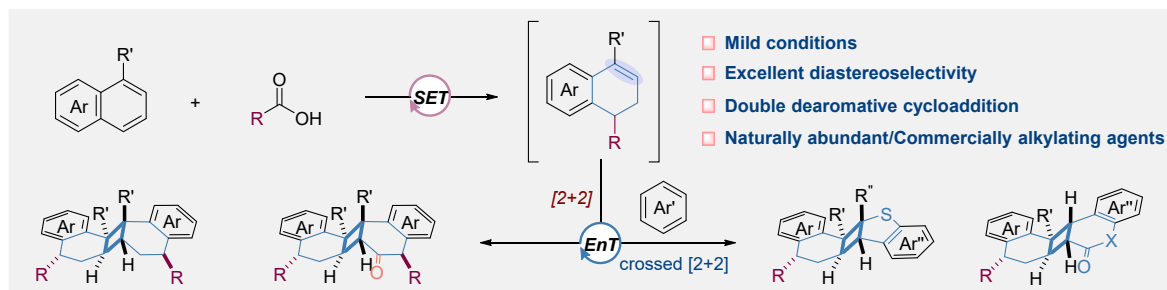


**Fig. 1.** Divergent construction of cyclobutane-fused pentacyclic scaffolds

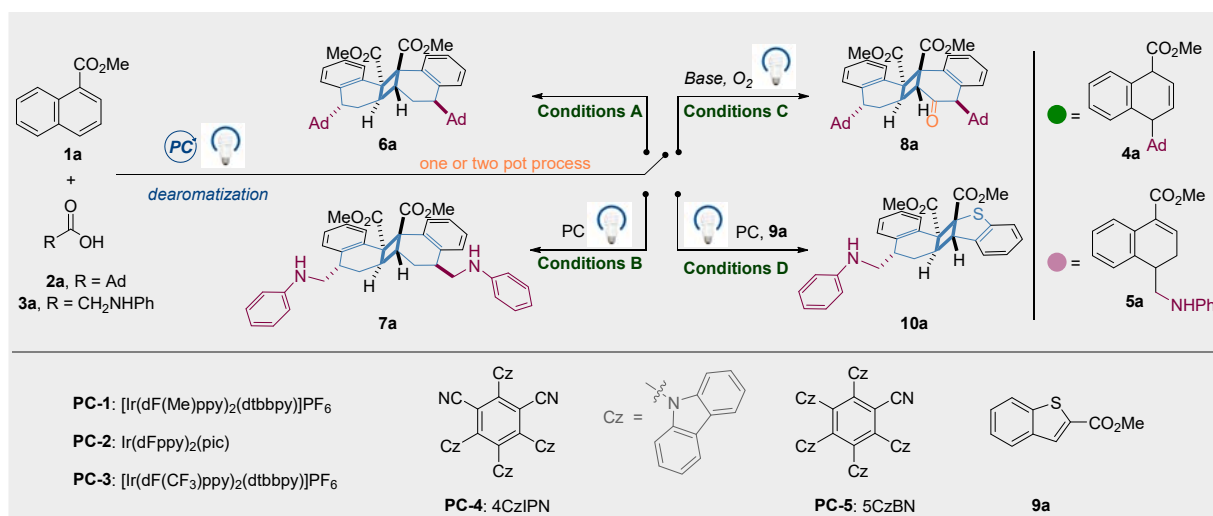
During the past decade, photo-induced dearomatization<sup>[6]</sup> has witnessed rapid advancements owing to the introduction of three-dimensional complexity from basic two-dimensional precursors. In this context, as efficient chemical processes, energy-transfer-enabled dearomative cycloaddition reactions have received considerable attention, as this approach demonstrates the ability to realize molecular diversity in one step.<sup>[6e, 7]</sup> Compared with non-aromatic partners in photocatalytic dearomatization,<sup>[8]</sup> aromatic partners are still scarce due to the inherent stability of aromatic compounds.<sup>[9]</sup> Taking advantage of intramolecular reactions, You<sup>[10]</sup> and Yin<sup>[11]</sup> have developed photo-induced intramolecular dearomative [4+2] or [2+2] cycloaddition of indole derivatives bearing a pendant aromatic ring (Fig. 1B). Compared with intramolecular dearomatization reactions,<sup>[8d, 12]</sup> the intermolecular variants<sup>[8a, 8c, 13]</sup> are more flexible to increase the structural diversity of target dearomative products. Under ultraviolet irradiation, photodimerization of anthracenes has been developed as one of the limited examples of intermolecular double dearomative cycloaddition.<sup>[14]</sup> Intrigued by the ability of visible-light-induced dearomative cycloadditions to construct structurally diverse polycyclic molecular structures, we hypothesized that the intermolecular double dearomative cycloaddition of two arene units beyond anthracenes might be implemented in the presence of visible light and photocatalyst. However, intermolecular dearomatization remains a great challenge due to the issues of regio- and stereoselectivities control coupled with unfavorable entropy decrease. Stemming from reported works on photoredox intermolecular dearomatization between naphthalenes and  $\alpha$ -amino acids by You<sup>[13c]</sup> and our group<sup>[13b]</sup> (Fig. 1C), we questioned whether double dearomative cycloaddition could be achieved with the help of an alkyl radical towards a cascade hydroalkylative dearomatization/cycloaddition forming unusual cyclobutane-fused rings from two arene units (Fig. 1D).

Inspired by these pioneering works and based on the continuation of our recent studies on divergent olefin transformations<sup>[15]</sup> and photocatalytic aminoalkylation,<sup>[13b]</sup> we herein demonstrated the divergent construction of functionalized cyclobutane-fused 2D/3D pentacyclic scaffolds by a visible-light-promoted intermolecular double dearomative cycloaddition of arenes (Fig. 1D). These reactions commenced with photocatalytic 1,4-hydroalkylation via a SET process and were followed by alkene isomerization and EnT-enabled [2+2] cycloaddition. The intertwined SET/EnT processes provided a straightforward approach for accessing synthetically challenging (pseudo)-dimeric cyclobutane-fused 2D/3D polycyclic rings. Particularly, energy-transfer-mediated intermolecular double dearomative cycloaddition between naphthalenes and benzothiophenes was also realized, providing unprecedented polycyclic molecules that are difficult to access by ground-state transformations.

## Results and Discussion

The initial trial involved the one-pot reaction of methyl 1-naphthoate **1a** with 1-adamantanecarboxylic acid **2a** in the

Table 1. Optimization studies of divergent synthesis of cyclobutane-fused pentacyclic scaffolds



## A Optimization of one-pot reaction conditions

1a + 2a		PC, K <sub>2</sub> CO <sub>3</sub> , hv → 6a	
Entry	Conditions	Yield of 6a <sup>a</sup>	dr of 6a <sup>a</sup>
1	Conditions A	54%	> 95:5
2	DBU instead of K <sub>2</sub> CO <sub>3</sub>	20%	> 95:5
3	THF instead of DMSO	trace	--
4	Without PC-1	0	--
5	Without K <sub>2</sub> CO <sub>3</sub>	0	--
6	In the dark	0	--

Conditions A: **1a** (0.10 mmol), **2a** (0.15 mmol), K<sub>2</sub>CO<sub>3</sub> (0.40 eq.) and **PC-1** (1.5 mol%), DMSO (1 mL), blue LEDs, RT, 24 h.

## B Optimization of homo-dimerization reactions

1a + 3a		PC, base, hv → 7a	
		then DBU → 7a	
Entry	Conditions	Yield of 7a <sup>a</sup>	dr of 7a <sup>a</sup>
1	Conditions B	96%	> 95:5
2	<b>PC-4</b> instead of <b>PC-2</b>	35%	> 95:5
3	Sc(OTf) <sub>3</sub> instead of TFA	90%	> 95:5
4	Without LiBr	45%	> 95:5
5	Without TFA	23%	> 95:5
6	In the dark	0	--

Conditions B: **5a** was isolated by adding DBU (0.5 eq.). **5a** (0.10 mmol), **PC-2** (2.0 mol%), LiBr (2.0 eq.), TFA (1.0 eq.), MeCN (0.5 mL), blue LEDs, RT, 24 h.

## C Optimization of formal crossed [2+2] reactions

1a + 2a		PC, base, hv → 8a	
		Base, O <sub>2</sub> , hv → 8a	
Entry	Conditions	Yield of 8a <sup>a</sup>	dr of 8a <sup>a</sup>
1	Conditions C	45%	> 95:5
2	<b>PC-3</b> (2.0 mol%) was added	0	--
3	DMF instead of DMSO	26%	> 95:5
4	N <sub>2</sub> atmosphere	0	--
5	Without K <sub>2</sub> CO <sub>3</sub>	0	--
6	In the dark	0	--

Conditions C: **4a** was isolated using THF instead of DMSO in conditions A. **4a** (0.10 mmol), LiBr (2.0 eq.), K<sub>2</sub>CO<sub>3</sub> (1.0 eq.), DMSO (1 mL), blue LEDs (456 nm), RT, air, 24 h.

## D Optimization of crossed [2+2] reactions

1a + 3a		PC, base, hv → 10a	
		then DBU → 9a	
Entry	Conditions	Yield of 10a <sup>a</sup>	dr of 10a <sup>a</sup>
1	Conditions D	71%	> 95:5
2	THF instead of MeCN	51%	93:7
3	<b>9a</b> (3 eq.) was added	56%	> 95:5
4	Without LiBr	8%	--
5	Without PC	0	--
6	In the dark	0	--

Conditions D: **5a** was isolated by adding DBU (0.5 eq.). **5a** (0.10 mmol), **9a** (0.50 mmol), **PC-5** (2.0 mol%), LiBr (2.0 eq.), TFA (1.0 eq.), MeCN (0.5 mL), blue LEDs, RT, 18 h.

<sup>a</sup>Yields and the ratio of diastereomers were determined by GC-FID or <sup>1</sup>HNMR.

presence of the photocatalyst  $[\text{Ir}(\text{dF}(\text{Me})\text{ppy})_2(\text{dtbbpy})]\text{PF}_6$  (**PC-1**) under irradiation with blue LEDs at room temperature (Table 1A). To our delight, the desired cyclobutane-fused pentacyclic product **6a** was obtained in 54% yield with excellent diastereoselectivity (> 95:5 dr) (entry 1). Photosensitizers  $\text{Ir}(\text{dFppy})_2\text{pic}$  (**PC-2**),  $[\text{Ir}(\text{dF}(\text{CF}_3)\text{ppy})_2(\text{dtbbpy})]\text{PF}_6$  (**PC-3**), 4CzIPN (**PC-4**) and  $[\text{Ir}(\text{ppy})_2(\text{dtbbpy})]\text{PF}_6$  (**PC-6**) were less efficient or inefficient (Table S1, entries 2–5 in SI). By comparison, when DBU was used instead of  $\text{K}_2\text{CO}_3$ , the yield of **6a** dropped to 20% (entry 2). THF and  $\text{Et}_2\text{O}$  gave only trace amounts of product **6a** compared with DMSO as solvent (Table S1, entries 6 and 7). Meanwhile, the formation of a large amount of 1,4-addition product **4a** demonstrates that both reaction systems are not conducive to isomerization. The control experiments confirmed the necessity of photocatalyst, base, and visible light irradiation in this dearomative process (entries 4–6). Of note, the reaction system generated not only the target product **6a** but also unavoidable byproducts, including residual isomerization product **5b**, 1,2-addition product, and dialkylated side product. These competing pathways resulted in a moderate to somewhat low yield of the desired product **6a** (Table S1). Furthermore, increasing the loading of the photocatalyst and base did not show significant improvement (Table S2 in SI).

Subsequent efforts were focused on the optimization of the homo-dimerization reaction of **5a** (Table 1B). Surprisingly, the formation of the bridged product in our previous work<sup>[13b]</sup> was inhibited when trifluoroacetic acid (TFA) was added. The [2+2] cycloaddition product **7a** was generated instead in 96% yield with excellent diastereoselectivity in the presence of the photocatalyst **PC-2**, TFA, and LiBr (entry 1). **PC-3** also proved highly efficient at promoting the cycloaddition process (Table S3, entry 2). In contrast, **PC-4** and **PC-6** exhibited reduced catalytic activities (Table S3, entries 3 and 4). MeCN was identified as the optimal reaction solvent compared to DCM and MeOH (Table S3, entries 5 and 6). Moreover, Lewis acid  $\text{Sc}(\text{OTf})_3$  showed comparable activity to TFA (entry 3). Additionally, lower yields were obtained in the absence of TFA or LiBr (entries 5 and 6). No desired product was observed without photosensitizer or the irradiation of blue LEDs even if under thermal conditions (Table S3, entries 10–12).

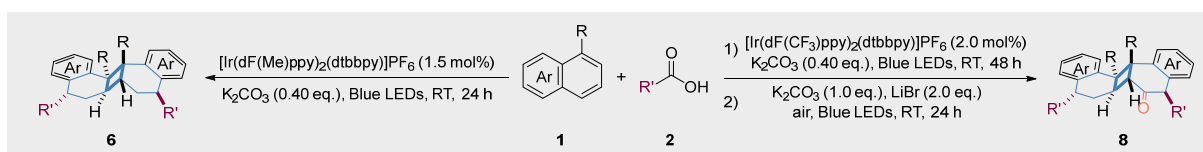
After realizing photocatalytic homo-dimerization reactions, the possibility of crossed [2+2] cycloaddition reaction of **4a** with green  $\text{O}_2$  as the oxygen source was further explored. Initial investigations were performed using isolated product **4a** (Table 1C). Unexpectedly, the formal crossed [2+2] cycloaddition product **8a** was obtained in 45% yield under irradiation with blue LEDs in an air atmosphere (entry 1). Of note, the addition of **PC-3** inhibited the formation of **8a**, only giving isomerization product **5a** and homo-dimer **6a** (entry 2). DMF gave only 26% yield compared with DMSO as solvent (entry 3). Other solvents gave a poor promoting effect on this cycloaddition reaction (Table S4, entry 1 vs entries 4–9 in SI). In addition, replacing the light sources (427 nm and 390 nm) proved inefficient (Table S4, entries 10 and 11). The control experiments showed that the absence of  $\text{O}_2$ , base, or visible light resulted in the complete inactivity of this transformation (entries 4–6). We didn't observe the dicarbonyl product **8a'** during the reaction process,

even when the reaction time was extended to 48 hours (Table S4). This might be due to steric hindrance, which prevents the formation of the dicarbonyl product.

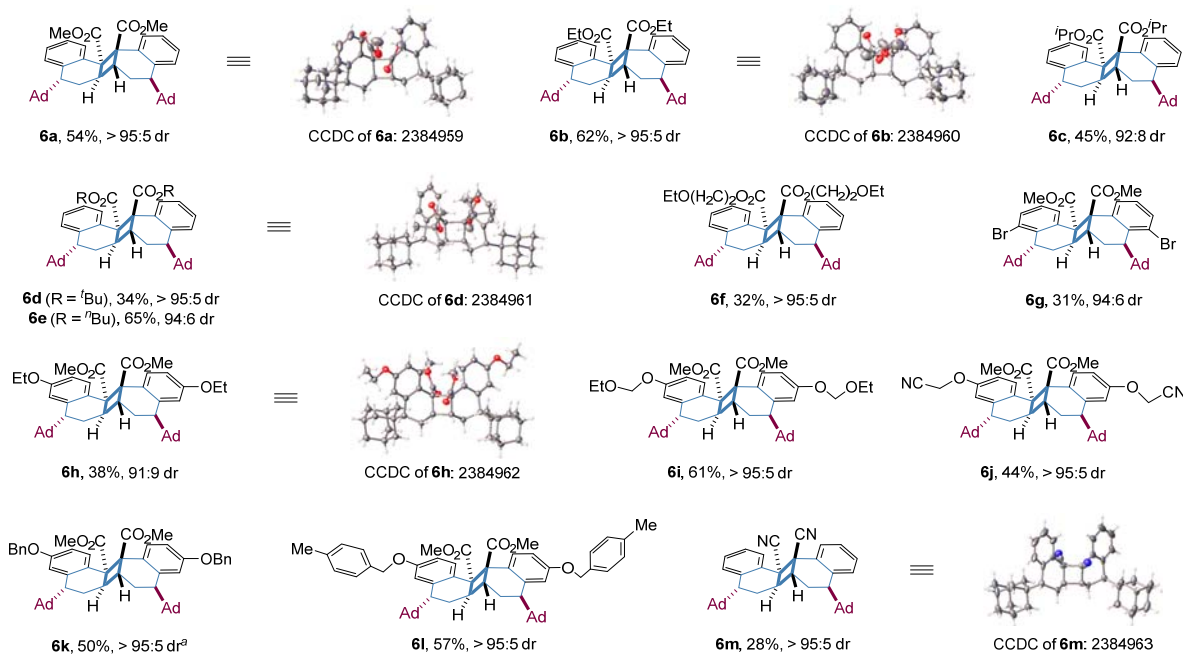
In addition, we also investigated intermolecular double dearomative cycloaddition between methyl 1-naphthoate **1a** and methyl benzo[*b*]thiophene-2-carboxylate **9a**. Upon exposure to blue LEDs, the desired intermolecular double dearomative [2+2] cycloaddition between **5a** and **9a** proceeded smoothly in the presence of organic photosensitizer 5CzBN (**PC-5**), LiBr, and TFA (Table 1D). The evaluation of solvent indicated that MeCN could serve as a more efficient solvent than THF (entries 1 and 2). In comparison, the addition of 3 eq. **9a** led to a lower yield (entry 3). The control experiments confirmed the necessity of both photocatalyst and visible light irradiation and indicated that LiBr is essential to the crossed [2+2] cycloaddition process (entries 4–6).

With the optimized reaction conditions in hand, the substrate scope for the one-pot reaction was investigated. The survey was initiated by probing the compatibility of various substitution patterns on the naphthalene moiety (Fig. 2A). Aromatic substrates with diverse ester moieties all performed well under the optimized conditions to provide dearomative cycloaddition products **6a–6f** in 32–65% yields with good diastereoselectivities. The structure of **6a** has been further confirmed by single crystal X-ray crystallography (CCDC: 2384959).<sup>[16]</sup> Moreover, the bromine-containing product at the C5 position (**6g**) could also be afforded. A variety of 6-alkoxy-substituted naphthyl esters proved effective substrates for this dearomative reaction, producing diversely substituted cyclobutane-fused pentacyclic products. A wide range of alkoxy substituents, including those containing alkyl, alkoxy, alkyl nitrile, and benzyl moieties, were well tolerated, providing target products (**6h–6l**) in moderate yields with high diastereoselectivities (> 95:5 dr). To our delight, substrate with –CN group also proceeded smoothly, affording the product **6m** with excellent diastereoselectivity (> 95:5 dr). The structure of **6m** has been further confirmed by single crystal X-ray crystallography (CCDC: 2384963).<sup>[16]</sup> Some unsuccessful heterocyclic substrates, such as quinolines or isoquinolines, were shown in Fig. S2 (See the Supplementary Information for more details).

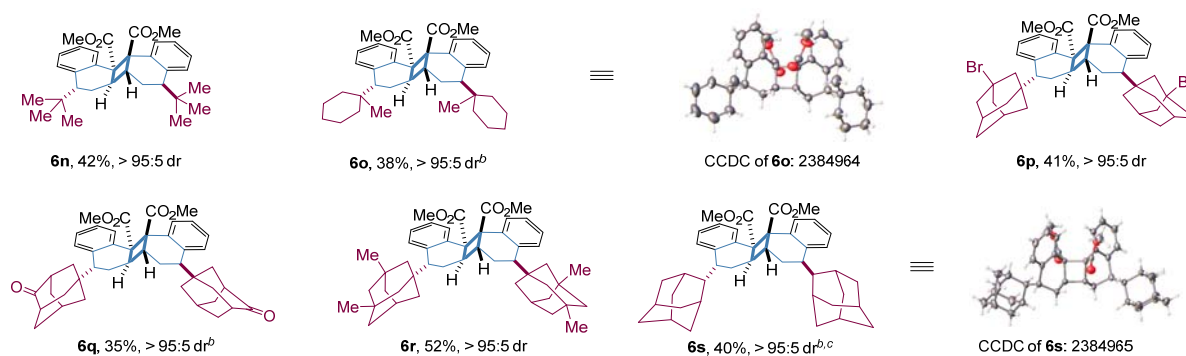
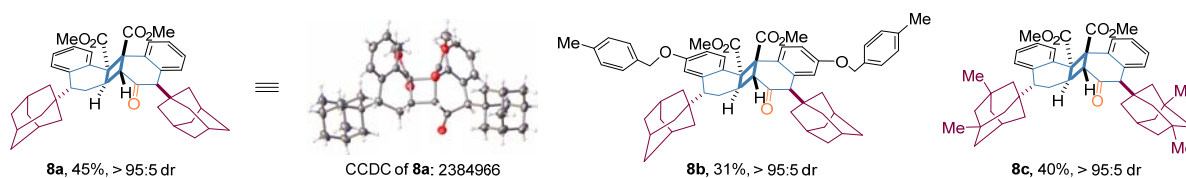
Next, diverse alkyl carboxylic acids were evaluated (Fig. 2B). Pivalic acid and 1-methylcyclohexanecarboxylic acid underwent decarboxylation and addition, providing the products with reasonable yields (**6n** and **6o**). A variety of substituted adamantanecarboxylic acids bearing various electron-withdrawing groups were investigated and could also be tolerated in this protocol (**6p** and **6q**). Dimethyladamantane-1-carboxylic acid was also compatible with the dearomative cycloaddition reaction thus providing cyclobutane-fused pentacyclic product **6r** in comparable yield. 2-Adamantanecarboxylic acid also worked smoothly, leading to polycyclic product **6s**. The structures of **6o** and **6s** have been further confirmed by single crystal X-ray crystallography (CCDC of **6o**: 2384964; CCDC of **6s**: 2384965).<sup>[16]</sup> Subsequently, an investigation into the substrate scope of formal crossed [2+2] reactions was conducted (Fig. 2C).



## A Aromatic hydrocarbon derivatives

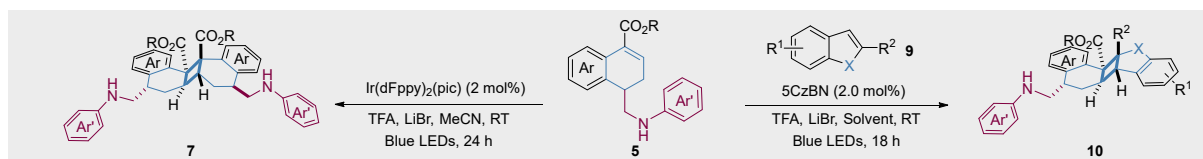
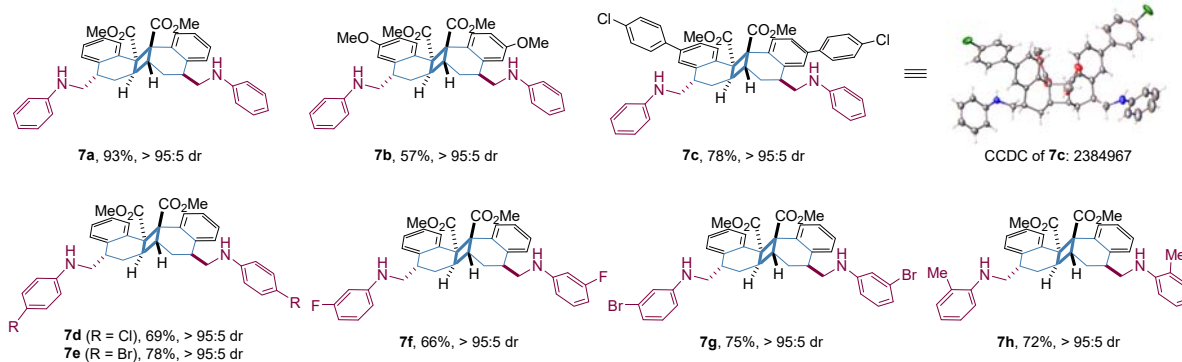
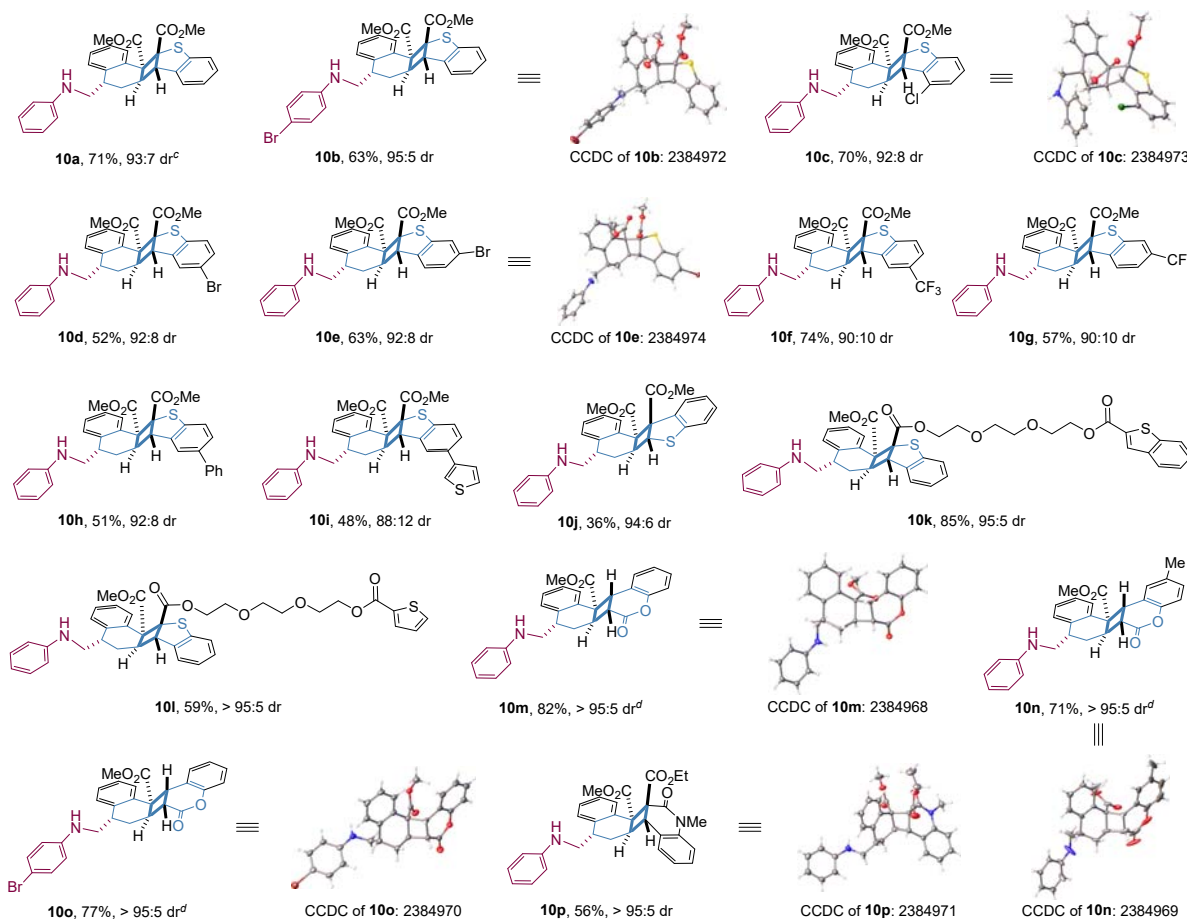


## B Carboxylic acid derivatives

C Formal crossed [2+2] products<sup>d</sup>

Conditions A: **1** (0.20 mmol), **2** (0.30 mmol), K<sub>2</sub>CO<sub>3</sub> (0.40 eq.), [Ir(dF(Me)ppy)<sub>2</sub>(dtbbpy)]PF<sub>6</sub> (1.5 mol%), DMSO (2 mL), RT, 24 h. <sup>a</sup>48 h. <sup>b</sup>**2** (0.30 mmol), K<sub>2</sub>CO<sub>3</sub> (0.40 eq.), PC were added twice every 24 h, 48 h in total. <sup>c</sup>4CzIPN (**PC-4**) was used as photocatalyst. <sup>d</sup>Conditions C: **1** (0.20 mmol), **2** (0.60 mmol), K<sub>2</sub>CO<sub>3</sub> (0.40 eq.), [Ir(dF(CF<sub>3</sub>)ppy)<sub>2</sub>(dtbbpy)]PF<sub>6</sub> (2.0 mol%), THF (2 mL), RT, 48 h. Then **4** (0.10 mmol), K<sub>2</sub>CO<sub>3</sub> (1.0 eq.), LiBr (2.0 eq.), DMSO (1 mL), blue LEDs, RT, air, 24 h.

Fig. 2. Substrate scope of one-pot reactions and formal crossed [2+2] reactions

Scope of the homo-dimerization reactions<sup>a</sup>Scope of the cross-dimerization reactions<sup>b</sup>

<sup>a</sup>Conditions B: **5** (0.10 mmol),  $\text{Ir}(\text{dFppy})_2(\text{pic})$  (2.0 mol%), LiBr (2.0 eq.), TFA (1.0 eq.), MeCN (0.5 mL), blue LEDs, RT, 24 h. <sup>b</sup>Conditions D: **5** (0.10 mmol), **9** (0.50 mmol), 5CzBN (2.0 mol%), LiBr (2.0 eq.), TFA (1.0 eq.), THF (0.5 mL), blue LEDs, RT, 18 h. <sup>c</sup>MeCN (0.5 mL) was used as solvent. <sup>d</sup>TXT (5.0 mol%) was used instead of 5CzBN.

**Fig. 3.** Substrate scope of dimerization reactions and crossed [2+2] reactions

Carbonylated polycyclic product **8a** was successfully accessed as a single diastereoisomer in 45% yield. The structure and relative stereochemistry of **8a** were determined unambiguously by X-ray crystallography (CCDC: 2384966).<sup>[16]</sup> Remarkably, 6-alkoxy-substituted naphthyl ester (**11**) was also a viable substrate for this transform, affording the desired formal crossed [2+2] product **8b**. In addition, for the reaction with isolated 1,4-addition product **4c** bearing dimethyl substituted adamantane group, the corresponding cyclobutane-fused product **8c** could be obtained in moderate yield.

As shown at the top of Fig. 3, we examined the scope for the dimerization of isolated compound **5** for the construction of cyclobutane-fused pentacyclic products with amine alkyl groups. Isomerization product **5a** showed high reactivity, providing fused cyclic product **7a** in 93% yield and good diastereoselectivity. Furthermore, methoxyl or aryl substituted dearomative dimers **7b** and **7c** could also be accessed in reasonable yields. The presence of chlorine or bromine atom at the C4 position of the *N*-phenyl ring promoted the formation of **7d** or **7e** in good yields. And *meta*-F and *meta*-Br could also be tolerated (**7f** and **7g**). The *ortho*-methyl substituted anilino group showed comparable reactivity and excellent diastereoselectivity (> 95:5 dr, **7h**) during the dimerization. Some amino acid-derived substrates that did not apply to this transformation are presented in Fig. S3 (See the Supplementary Information for more details).

Subsequently, the generality of intermolecular double dearomative cycloaddition between naphthalenes and benzothiophenes was evaluated. For methyl benzothiophene carboxylate derivatives, the corresponding cyclobutane-fused 6-6-4-5-6-membered rings were obtained with good yields and diastereoselectivities (Fig. 3, bottom). Initial study with **9a** was carried out to give corresponding fused-ring product **10a** in 71% isolated yield. The substrate bearing 4-Br substituted anilino group was compatible with this [2+2] cycloaddition reaction (**10b**). In general, a variety of substituents bearing various electron-withdrawing groups (-Cl, -Br, and -CF<sub>3</sub>) at the 5, 6, or 7-position proved amenable to this transformation by providing products **10c-10g** in decent yields and good diastereoselectivities. X-ray structures of **10b**, **10c**, and **10e** were presented to confirm the configuration of the products (**10b**, CCDC: 2384972; **10c**, CCDC: 2384973; **10e**, CCDC: 2384974).<sup>[16]</sup> The variation of the electron-rich substituent (-Ph) at the 6-position of the benzothiophene ring was examined, delivering the pentacyclic product **10h** in 51% yield. Gratifyingly, the thiophenyl group at the 6-position of the benzothiophene ring showed good compatibility in the double dearomative cycloaddition (**10i**). In addition, methyl benzothiophene-3-carboxylate was also applied in this protocol (**10j**). The high-yield resulting single-isomer product **10k** indicates exceptional chemo- and regioselectivity. For the substrate containing both benzothiophene and thiophene moieties, the reaction occurred exclusively at the benzothiophene site (**10l**). Furthermore, a series of coumarins proved compatible with this protocol, providing a straightforward avenue to

2D/3D cyclobutane-fused 6–6–4–6–6-membered ring systems and more opportunities for further diversification. Some unsuccessful indole substrates have been shown in Fig. S4. Of note, 2-ester indole and *N*-methyl-2-ester indole underwent Michael addition with **5a** to afford products **10q** and **10r** in 66% and 54% yield, respectively. The structure of **10q** has been further confirmed by single crystal X-ray crystallography (CCDC of **10q**: 2447518)<sup>[16]</sup> (See the Supplementary Information for more details).

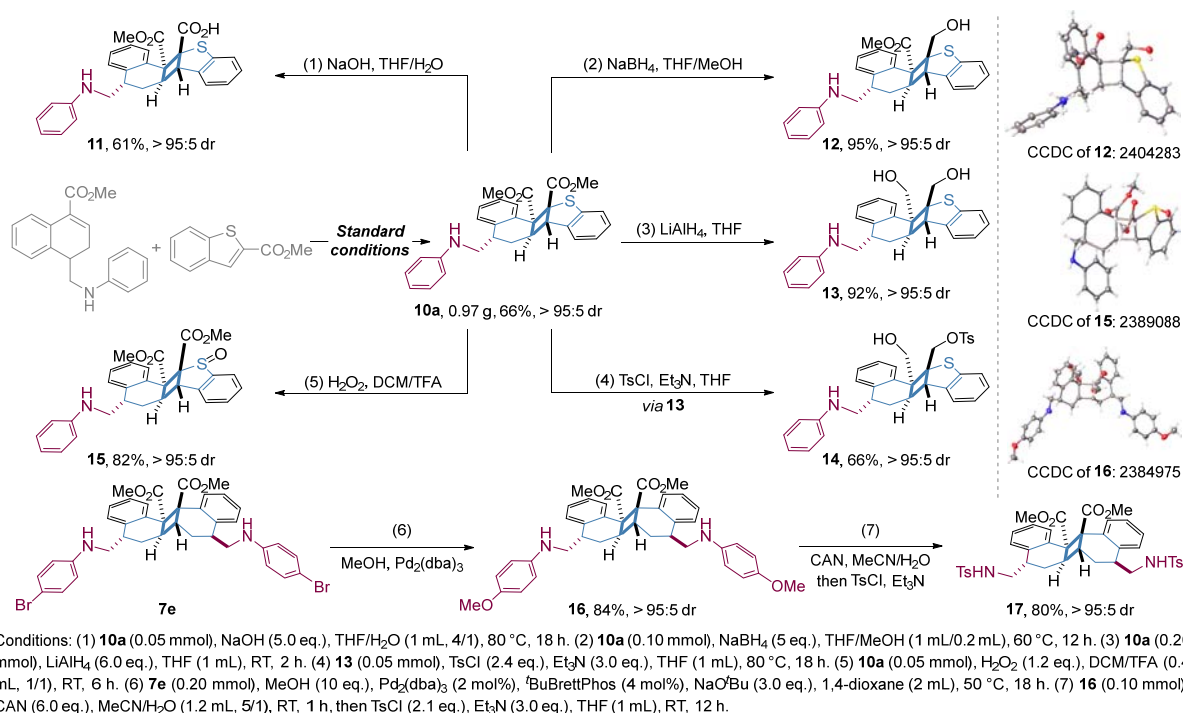


Fig. 4. Synthetic transformations

The developed double dearomative photocycloaddition protocol enables rapid access to highly functionalized cyclobutane-fused polycyclic molecules under mild conditions. These compounds serve as versatile building blocks, enabling further structural diversification through subsequent transformations. (Fig. 4). Initially, a gram scale experiment was successfully performed to provide cycloaddition product **10a** in 66% yield. Under alkaline hydrolysis conditions, monocarboxylic acid product **11** was obtained in moderate yield with maintaining excellent diastereoselectivity (>95:5 dr). With the addition of NaBH<sub>4</sub>, compound **10a** could be selectively reduced to give primary alcohol product **12**. Steric hindrance likely dictates the exclusive formation of hydrolysis product **11** and reduction product **12** at the ester group adjacent to the benzothiophene moiety. Furthermore, both ester groups of compound **10a** were readily reduced by LiAlH<sub>4</sub> to deliver the corresponding diol **13** in 92% yield. The transformation of compound **13** into mono-sulfonate **14** proceeded smoothly. The chemoselective oxidation of **10a** was successfully carried out to give sulfoxide **15** in 82% yield. In addition, product **16** bearing a good deprotection *p*-methoxyphenyl (PMP) group was

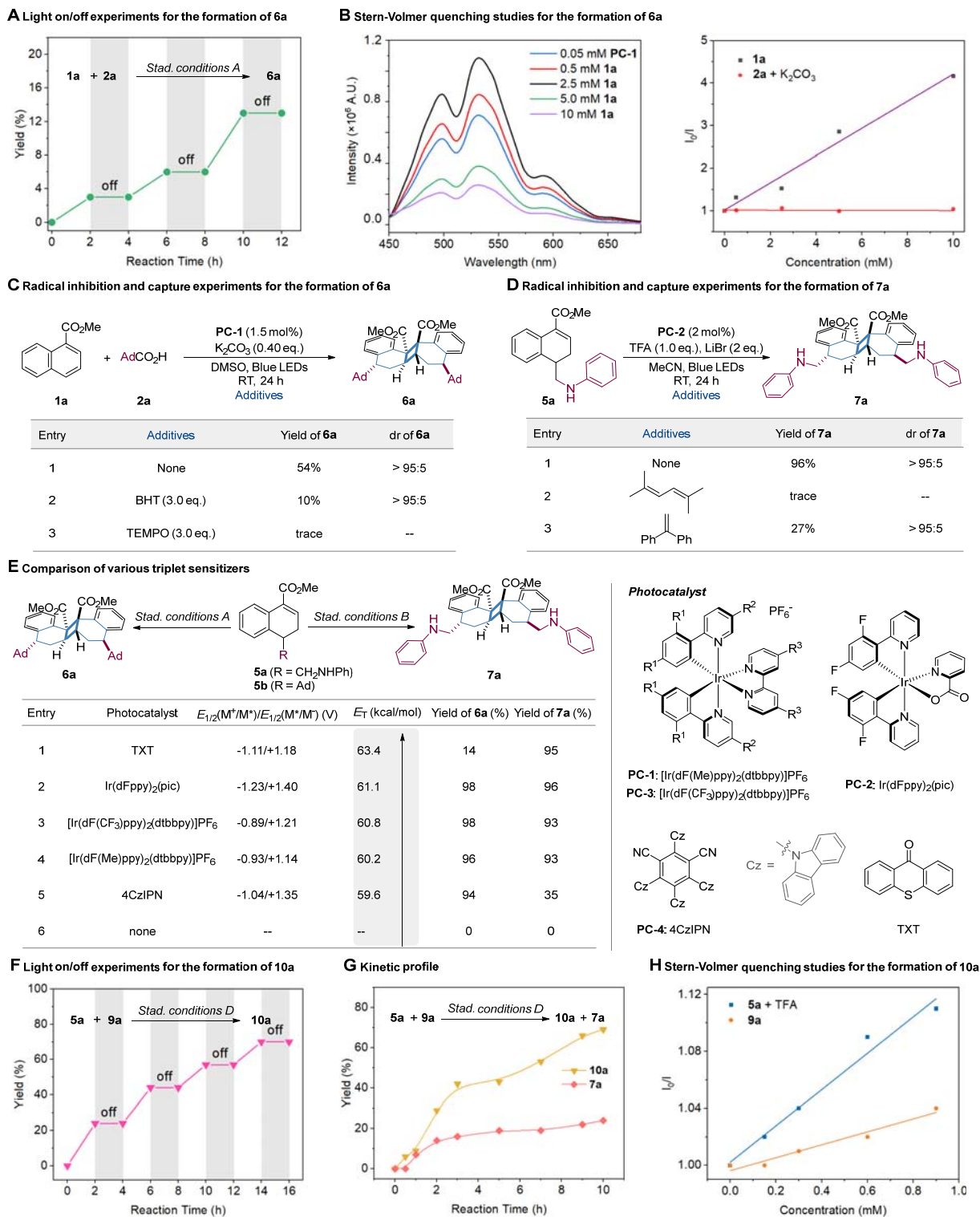


Fig. 5. Mechanistic studies

synthesized under Pd catalysis.<sup>[17]</sup> Corresponding Ts-protected product **17** could be produced in 80% yield through the oxidative deprotection of the PMP group on the nitrogen and subsequent protection by tosyl chloride. X-ray structures of products **12**, **15**, and **16** were presented to confirm the configuration of these products (CCDC of **12**: 2404283; CCDC of **15**: 2389088; CCDC of **16**: 2384975).<sup>[16]</sup> These successful transformations of various functional groups further demonstrated the potential applicability of these cyclobutane-fused polycyclic motifs.

To gain detailed insights into the mechanism of our developed double dearomative photocycloaddition reaction, combined experimental and computational studies were performed (Fig.s 5 and 6). Firstly, light on/off experiments verified that constant illumination is an essential element for the formation of product **6a** (Fig. 5A). To further clarify the interaction details between photocatalyst and substrate **1a** or **2a**, the fluorescence quenching experiments of [Ir(dF(Me)ppy)<sub>2</sub>(dtbbpy)PF<sub>6</sub>] with **1a** and [**2a** + K<sub>2</sub>CO<sub>3</sub>] mixture were accomplished, respectively. The Stern-Volmer analysis suggested that the luminescence emission of photocatalyst PC\* was quenched more efficiently by **1a** than **2a** (Fig. 5B). It implies that an oxidative quenching is probably involved in this photocatalytic quenching cycle, which is different from the previous reductive quenching mechanism.<sup>[13b]</sup> Meanwhile, this reaction was hindered by the addition of radical inhibitor TEMPO or BHT, which hints at the radical nature of this dearomative process (Fig. 5C, entries 1–3). And the observation of TEMPO-adduct by ESI-HRMS suggests that the adamantyl radical intermediate is likely involved in the reaction (Fig. S7 in SI). In addition, the yield of **7a** decreased sharply in the presence of known triplet quenchers, such as 2,5-dimethylhexa-2,4-diene or 1,1-diphenylethylene (Fig. 5D, entries 1–3). These suggest that the excited triplet state intermediate is probably involved in this cycloaddition process. To explore which step the photosensitizer is involved in energy transfer, the cycloaddition reactions of isolated **5a** and **5b** were examined respectively using different organic- and metal-based photocatalysts (Fig. 5E). No obvious linear correlation relationship between yield and triplet energy was observed. It showed the “sweet spot” at 59–61 kcal mol<sup>-1</sup> for **6a** (entries 2–5), and 60–61 kcal mol<sup>-1</sup> for **7a** (entries 2–4). These results implied that an energy transfer (EnT) process is likely to occur in the dearomative cycloaddition. Subsequent efforts were directed towards corroborating the postulated triplet-energy-transfer mechanism for crossed dimerization reactions between **5a** and **9a**. The light on/off experiments are consistent with the corresponding control reaction, showing that the exclusion of light failed to deliver target product **10a** (Fig. 5E and Table 1D, entry 6). Moreover, the kinetic profile of a standard reaction of **5a** and **9a** demonstrated rapid progression without induction periods (Fig. 5G). For reactive species that initiates the cycloaddition, Stern–Volmer quenching studies suggested an energy transfer event between the excited-state photosensitizer and [**5a** + TFA] was involved (Fig. 5H).

Based on previous literatures<sup>[18]</sup> and performed mechanistic experiments, a plausible mechanism is proposed (Fig.

6A) and the corresponding Gibbs energy profile for the dearomative [2+2] cycloaddition to form product **6a** calculated using density functional theory (DFT) is shown (Fig. 6B). This reaction commences with the activation of photocatalyst Ir<sup>III</sup> to generate the excited state \*Ir<sup>III</sup>. Naphthyl ester (**1a**, E<sup>0</sup><sub>red</sub> = 1.89 V vs. SCE) is sensitized by the lowest triplet excited state (\*Ir<sup>III</sup>), which is from visible-light photoexcitation of Ir<sup>III</sup>, giving the formation of the triplet state of naphthyl ester <sup>3</sup>[**1a**], which lies 60.8 kcal/mol above its ground state. Subsequently, <sup>3</sup>[**1a**] is reduced by single electron transfer (SET) from excited \*Ir<sup>III</sup> within an oxidation quenching cycle to yield intermediate **I** and Ir<sup>IV</sup>. The formation of radical anionic intermediate **I** is exergonic, as this species is 55.8 kcal/mol downhill of substrate **1a**. Subsequent protonation of **I** by 1-adamantanecarboxylic acid gives rise to carbon-centered radical intermediate **II**, which is 9.4 kcal/mol uphill of **I**. Next, single-electron oxidation of deprotonated and decarboxylated **2a** by the oxidative Ir<sup>IV</sup> affords nucleophilic alkyl radical **III** and simultaneously regenerates the photocatalyst. Radical–radical coupling follows to forge a new C–C bond with the concomitant formation of 1,4-dihydro naphthalene **4a**. Due to both electronic and steric effects, the alkylation of intermediate **II** occurs selectively at the C4 position. This step is highly exergonic, by 50.0 kcal/mol, as a strong C–C bond is formed. The isomerization of **4a** occurs to give an almost isoenergetic product **5b**, which can undergo an efficient triplet energy transfer (EnT) from photoexcited PC\* to give triplet-state <sup>3</sup>[**5b**] that is 57.7 kcal/mol above its ground state. Subsequently, <sup>3</sup>[**5b**] can complex and react with another molecule of **5b** to undergo stepwise [2+2] cycloaddition, forming diradical intermediate **IV**. Intersystem crossing of the resultant triplet 1,4-diradical **IV** to its singlet state allows subsequent barrierless *trans*-selective radical–radical recombination to deliver the cycloaddition product **6a**, which is highly exergonic, at -147.6 kcal/mol relative to the starting material **1a**.

The diastereo- and regioselectivity determining step arises from the first C–C bond formation event in the triplet state and was studied using DFT (SI sections 2.8.5 and 2.8.6). Spin density plots of <sup>3</sup>[**5b**] indicate that the β-carbon has the highest radical characteristic (Figure S33) and will attack the neutral substrate **5b** from this carbon atom. After detailed conformational considerations (with adamantyl groups either axial or equatorial, Figure S34), the head-to-head (β-carbon of <sup>3</sup>[**5b**] attacking β-carbon of **5b**) *anti*-addition with key H atoms all *trans* (<sup>3</sup>[**TS1**], Fig. 6B) has the lowest barrier of 3.5 kcal/mol; the *anti*-addition where the key H atoms are *cis*, *trans* (<sup>3</sup>[**TS1a**], Fig. 6B) has a barrier that is 13.7 kcal/mol higher. On the other hand, the *syn*-addition where the key H atoms are *cis*, *cis* (<sup>3</sup>[**TS1s**], Fig. 6B) has a barrier that is 5.6 kcal/mol higher. The regioisomeric TS with head-to-tail addition (<sup>3</sup>[**TS1r**], Fig. 6B and Figure S35) has a barrier that is 8.9 kcal/mol higher than <sup>3</sup>[**TS1**]. These activation barrier differences would predict a *dr* ratio of > 99:1, in good agreement with the experimentally observed value of 95:5. This stereo- and regioselectivity outcome (head-to-head *anti*-addition) also agrees with that observed in the one-electron oxidant promoted cyclobutanation of unsymmetrical olefins.<sup>[19]</sup>

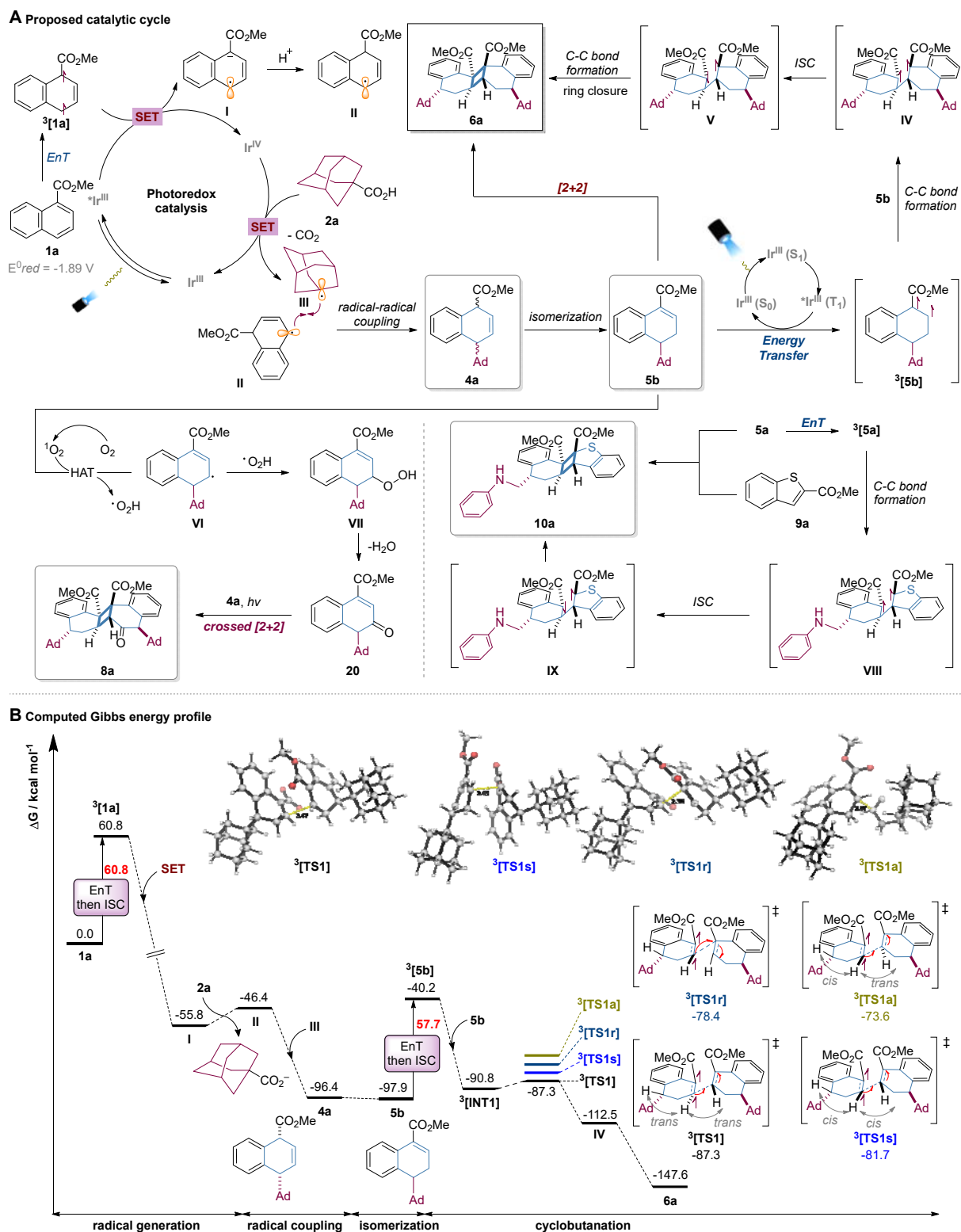


**Fig. 6.** Proposed mechanism and computed Gibbs energy profile at SMD(DMSO)-M06-2X/def2TZVP//M06-2X/def2-SVP level of theory.

To understand the reaction mechanism for the formation of carbonylated polycyclic product **8**, further DFT studies were performed (SI section 2.8.8). The Gibbs energy for the formation of structure **20** is shown in Figure S36. Briefly, molecular oxygen ( $^3\text{O}_2$ ) undergoes energy transfer to yield the singlet oxygen ( $^1\text{O}_2$ ) under visible light irradiation.<sup>[20]</sup> This highly active singlet oxygen ( $^1\text{O}_2$ ) can abstract a hydrogen atom from **5b** to yield the allyl radical **VI** and hydroperoxyl radical  $\cdot\text{O}_2\text{H}$  (downhill by 11.6 kcal/mol), which will recombine to give peroxide **VII**. This process is exergonic and thermodynamically favorable, as a strong C–C bond is formed, with **VII** lying 32.2 kcal/mol downhill of **VI**. Subsequent base-assisted deprotonation yields acetophenone **20** from **VII**, with a thermally accessible barrier of 18.7 kcal/mol (Figure S37). An alternative mechanism based on the proposal for the selective C–H bond aerobic oxidation<sup>[21]</sup> was deemed unsuitable, as the addition of oxygen is less favorable than the addition of hydroperoxyl radical  $\cdot\text{O}_2\text{H}$  to radical **VI** (Figure S36). Further crossed [2+2] cycloaddition between **20** and **4a** under irradiation of light leads to carbonylated polycyclic product **8a**. For crossed [2+2] cycloaddition reaction between **5a** and **9a**, a similar mechanism occurs where visible light excited 5CzBN sensitizes **5a** via EnT, and the resulting triplet state  $^3[5a]$  approaches **9a** to form a diradical species **VIII**. Intermediate **VIII** undergoes intersystem crossing (ISC) (intermediate **IX**) and ring closure to deliver the crossed cycloaddition product **10a**.

## Conclusion

In conclusion, we have developed a divergent synthetic protocol for constructing the structurally diverse cyclobutane-fused pentacyclic scaffolds via a photocatalytic double dearomatization. This strategy provides a straightforward avenue to cyclobutane-fused 2D/3D pentacyclic systems (6–6–4–6–6 and 6–6–4–5–6-membered fused rings). Extremely high structural complexity was directly elaborated from readily two-dimensional (2D) aromatic compounds and available carboxylic acids via intertwined SET/EnT processes. High regioselectivities and excellent diastereoselectivities, which are challenging within the intermolecular dearomative cycloaddition arsenal, have been observed. Combined experimental and computational mechanistic studies unravel the reaction mechanism and point to the first C–C bond formation as the diastereo- and regioselectivity step. Compared to the conventional cycloaddition reactions, using aromatics as reactants and harnessing consecutive transformations, this protocol expands the chemical space for the construction of complex cyclobutanes via dearomative strategies. Given the ubiquity of cyclobutane-fused 2D/3D rings in drug candidates, we expect this transformation to provide a new platform for the facile synthesis of cyclobutane-fused 2D/3D pentacyclic scaffolds.

## Acknowledgments

Financial support from Dalian Institute of Chemical Physics (DICPI201902) and the National Natural Science Foundation of China (22371275 and 22071239) is acknowledged. X. Z. acknowledges the funding support from the Chinese University of Hong Kong (CUHK) under the Vice-Chancellor Early Career Professorship Scheme Research Startup Fund (Project Code 4933634) and Research Startup Matching Support (Project Code 5501779).

#### Declaration of interests

The authors declare no competing interests.

#### Data and materials availability

The X-ray crystallographic data for compounds have been deposited in the Cambridge Crystallographic Data Centre (CCDC). All other data are available in the supplementary materials.

**Keywords:** dearomatization; photocatalysis; cycloaddition; polycyclic scaffolds; cyclobutane

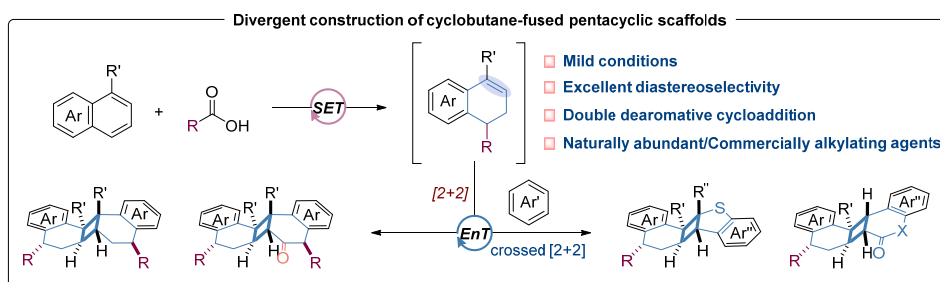
#### References

- [1] a) S. A. Snyder, A. M. ElSohly, F. Kontes, *Nat. Prod. Rep.* **2011**, *28*, 897; b) J. Sun, H. Yang, W. Tang, *Chem. Soc. Rev.* **2021**, *50*, 2320; c) Y. Fan, J. Shen, Z. Liu, K. Xia, W. Zhu, P. Fu, *Nat. Prod. Rep.* **2022**, *39*, 1305; d) P. Yang, Q. Jia, S. Song, X. Huang, *Nat. Prod. Rep.* **2023**, *40*, 1094.
- [2] B.-X. Zhao, Y. Wang, C. Li, G.-C. Wang, X.-J. Huang, C.-L. Fan, Q.-M. Li, H.-J. Zhu, W.-M. Chen, W.-C. Ye, *Tetrahedron Lett.* **2013**, *54*, 4708.
- [3] M. E. Flores-Giubi, M. J. Durán-Peña, J. M. Botubol-Ares, F. Escobar-Montaño, D. Zorrilla, A. J. Macías-Sánchez, R. Hernández-Galán, *J. Nat. Prod.* **2017**, *80*, 2161.
- [4] W. Wang, Y. Tang, Y. Liu, L. Yuan, J. Wang, B. Lin, D. Zhou, L. Sun, R. Huang, G. Chen, N. Li, *Org. Chem. Front.* **2019**, *6*, 2850.
- [5] K.-i. Nakashima, M. Oyama, T. Ito, Y. Akao, J. R. Witono, D. Darnaedi, T. Tanaka, J. Murata, M. Inuma, *Tetrahedron* **2012**, *68*, 2421.
- [6] a) C. J. Huck, D. Sarlah, *Chem* **2020**, *6*, 1589; b) M. Okumura, D. Sarlah, *Eur. J. Org. Chem.* **2020**, *2020*, 1259; c) Y.-Z. Cheng, Z. Feng, X. Zhang, S.-L. You, *Chem. Soc. Rev.* **2022**, *51*, 2145; d) C. J. Huck, Y. D. Boyko, D. Sarlah, *Nat. Prod. Rep.* **2022**, *39*, 2231; e) M. Zhu, X. Zhang, C. Zheng, S.-L. You, *Acc. Chem. Res.* **2022**, *55*, 2510; f) D.-H. Liu, J. Ma, *Angew. Chem. Int. Ed.* **2024**, *63*, e202402819.
- [7] a) F. Strieth-Kalthoff, M. J. James, M. Teders, L. Pitzer, F. Glorius, *Chem. Soc. Rev.* **2018**, *47*, 7190; b) Q. Q. Zhou, Y. Q. Zou, L. Q. Lu, W. J. Xiao, *Angew. Chem. Int. Ed.* **2018**, *58*, 1586; c) J. Großkopf, T. Kratz, T. Rigotti, T. Bach, *Chem. Rev.* **2022**, *122*, 1626; d) S. Dutta, J. E. Erchinger, F. Strieth-Kalthoff, R. Kleinmans, F. Glorius, *Chem.*

- Soc. Rev.* **2024**, *53*, 1068.
- [8] a) J. Ma, S. Chen, P. Bellotti, R. Guo, F. Schäfer, A. Heusler, X. Zhang, C. Daniliuc, M. K. Brown, K. N. Houk, F. Glorius, *Science* **2021**, *371*, 1338; b) R. Guo, S. Adak, P. Bellotti, X. Gao, W. W. Smith, S. N. Le, J. Ma, K. N. Houk, F. Glorius, S. Chen, M. K. Brown, *J. Am. Chem. Soc.* **2022**, *144*, 17680; c) J. Ma, S. Chen, P. Bellotti, T. Wagener, C. Daniliuc, K. N. Houk, F. Glorius, *Nat. Catal.* **2022**, *5*, 405; d) R. Kleinmans, S. Dutta, K. Ozols, H. Shao, F. Schäfer, R. E. Thielemann, H. T. Chan, C. G. Daniliuc, K. N. Houk, F. Glorius, *J. Am. Chem. Soc.* **2023**, *145*, 12324.
- [9] X. Liu, J. Zhang, *Chem. Eur. J.* **2025**, *31*, e202404640.
- [10] M. Zhu, H. Xu, X. Zhang, C. Zheng, S. L. You, *Angew. Chem. Int. Ed.* **2021**, *133*, 7112.
- [11] G. Zhen, G. Zeng, K. Jiang, F. Wang, X. Cao, B. Yin, *Chem. Eur. J.* **2023**, *29*, e202203217.
- [12] a) M. J. James, J. L. Schwarz, F. Strieth-Kalthoff, B. Wibbeling, F. Glorius, *J. Am. Chem. Soc.* **2018**, *140*, 8624; b) M. Zhu, C. Zheng, X. Zhang, S.-L. You, *J. Am. Chem. Soc.* **2019**, *141*, 2636; c) M. S. Oderinde, E. Mao, A. Ramirez, J. Pawluczyk, C. Jorge, L. A. M. Cornelius, J. Kempson, M. Vetrichelvan, M. Pitchai, A. Gupta, A. K. Gupta, N. A. Meanwell, A. Mathur, T. G. M. Dhar, *J. Am. Chem. Soc.* **2020**, *142*, 3094; d) Z. Zhang, D. Yi, M. Zhang, J. Wei, J. Lu, L. Yang, J. Wang, N. Hao, X. Pan, S. Zhang, S. Wei, Q. Fu, *ACS Catal.* **2020**, *10*, 10149; e) M. Zhu, X. Zhang, C. Zheng, S.-L. You, *ACS Catal.* **2020**, *10*, 12618; f) X. P. Mu, Y. H. Li, N. Zheng, J. Y. Long, S. J. Chen, B. Y. Liu, C. B. Zhao, Z. Yang, *Angew. Chem. Int. Ed.* **2021**, *60*, 11211; g) M. Zhu, X.-L. Huang, S. Sun, C. Zheng, S.-L. You, *J. Am. Chem. Soc.* **2021**, *143*, 13441; h) P. Yan, S. Stegbauer, Q. Wu, E. Kolodzeiski, C. J. Stein, P. Lu, T. Bach, *Angew. Chem. Int. Ed.* **2024**, *63*, e202318126.
- [13] a) J. A. Leitch, T. Rogova, F. Duarte, D. J. Dixon, *Angew. Chem. Int. Ed.* **2020**, *59*, 4121; b) T. T. Song, Y. K. Mei, Y. Liu, X. Y. Wang, S. Y. Guo, D. W. Ji, B. Wan, W. Yuan, Q. A. Chen, *Angew. Chem. Int. Ed.* **2024**, *63*, e202314304; c) Y. Z. Cheng, X. L. Huang, W. H. Zhuang, Q. R. Zhao, X. Zhang, T. S. Mei, S. L. You, *Angew. Chem. Int. Ed.* **2020**, *59*, 18062.
- [14] a) H.-D. Becker, *Chem. Rev.* **1993**, *93*, 145; b) H. Bouas-Laurent, A. Castellan, J.-P. L. Desvergne, René, *Chem. Soc. Rev.* **2000**, *29*, 43; c) H. Bouas-Laurent, J.-P. Desvergne, A. Castellan, R. Lapouyade, *Chem. Soc. Rev.* **2001**, *30*, 248.
- [15] a) Y.-C. Hu, D.-W. Ji, C.-Y. Zhao, H. Zheng, Q.-A. Chen, *Angew. Chem. Int. Ed.* **2019**, *58*, 5438; b) C.-S. Kuai, D.-W. Ji, C.-Y. Zhao, H. Liu, Y.-C. Hu, Q.-A. Chen, *Angew. Chem. Int. Ed.* **2020**, *59*, 19115; c) W.-S. Jiang, D.-W. Ji, W.-S. Zhang, G. Zhang, X.-T. Min, Y.-C. Hu, X.-L. Jiang, Q.-A. Chen, *Angew. Chem. Int. Ed.* **2021**, *60*, 8321; d) G. Zhang, C.-Y. Zhao, X.-T. Min, Y. Li, X.-X. Zhang, H. Liu, D.-W. Ji, Y.-C. Hu, Q.-A. Chen, *Nat. Catal.* **2022**, *5*, 708; e) W.-S. Zhang, D.-W. Ji, Y. Yang, T.-T. Song, G. Zhang, X.-Y. Wang, Q.-A. Chen, *Nat. Commun.* **2023**, *14*, 7087; f) S.-Y. Guo, Y.-P. Liu, J.-S. Huang, L.-B. He, G.-C. He, D.-W. Ji, B. Wan, Q.-A. Chen, *Nat. Commun.* **2024**, *15*, 6102;

- g) B. C. Zhou, B. Z. Chen, T. T. Song, Y. Yang, L. M. Zhang, D. W. Ji, B. Wan, Q. A. Chen, *Angew. Chem. Int. Ed.* **2024**, *63*, e202317299.
- [16] Deposition Numbers 2384959 (for **6a**), 2384960 (for **6b**), 2384961 (for **6d**), 2384962 (for **6h**), 2384963 (for **6m**), 2384964 (for **6o**), 2384965 (for **6s**), 2384966 (for **8a**), 2384967 (for **7c**), 2384972 (for **10b**), 2384973 (for **10c**), 2384974 (for **10e**), 2384968 (for **10m**), 2384969 (for **10n**), 2384970 (for **10o**), 2384971 (for **10p**), 2447518 (for **10q**), 2404283 (for **12**), 2389088 (for **15**) and 2384975 (for **16**) contain the supplementary crystallographic data for this paper. These data are provided free of charge by the Cambridge Crystallographic Data Centre and Fachinformationszentrum Karlsruhe Access Structures service.
- [17] C. Xi, Y. Jiang, X. Yang, *Tetrahedron Lett.* **2005**, *46*, 3909.
- [18] a) A. Chatterjee, B. König, *Angew. Chem. Int. Ed.* **2019**, *58*, 14289; b) E. Y. K. Tan, A. S. Mat Lani, W. Sow, Y. Liu, H. Li, S. Chiba, *Angew. Chem. Int. Ed.* **2023**, *62*, e202309764.
- [19] a) I. Colomer, R. Coura Barcelos, T. J. Donohoe, *Angew. Chem. Int. Ed.* **2016**, *55*, 4748; b) X. Zhang, R. S. Paton, *Chem. Sci.* **2020**, *11*, 9309.
- [20] J. Zhang, T. Hu, H. Lv, C. Dong, *Int. J. Hydrogen Energy* **2016**, *41*, 12722.
- [21] P. Huang, Y. Xu, H. Song, J. Wang, J. Wang, J. Li, B. Sun, C. Jin, *Green Chem.* **2024**, *26*, 9241.

## Table of Contents



A divergent synthetic strategy has been developed to construct cyclobutane-fused pentacyclic scaffolds via a photocatalytic intermolecular double dearomative cycloaddition of arenes.